Advances in the Fabrication of Biomaterials for Gradient Tissue Engineering

Chunching Li,[1†] Liliang Ouyang,[1†] James P. K. Armstrong[1*] & Molly M. Stevens[1*]

[1] Department of Materials, Department of Bioengineering and Institute of Biomedical Engineering, Imperial College London, Prince Consort Road, London, SW7 2AZ, United Kingdom

[†] These authors contributed equally, * Correspondence: m.stevens@imperial.ac.uk (M. M. Stevens) and james.armstrong@imperial.ac.uk (J. P. K. Armstrong).

Keywords: gradient, biofabrication, tissue engineering, heterogeneity

Additional Author Information

L. Ouyang: Website (https://www.linkedin.com/in/liliang-ouyang-85724369/), Twitter (@LiliangOuyang), ORCID (0000-0003-4177-8698)

J.P.K. Armstrong: Website (www.linkedin.com/in/james-armstrong-08480048/), Twitter (@jrmstrng), ORCID (0000-0002-0599-0643)

M.M. Stevens: Website (www.stevensgroup.org), Twitter (@UKRMP_Smart), ORCID (0000-0002-7335-266X)

Abstract

Natural tissues and organs exhibit an array of spatial gradients, from the polarized neural tube during embryonic development to the osteochondral interface present at articulating joints. The strong structure-function relationships in these heterogeneous tissues have sparked intensive research into the development of methods that can replicate physiological gradients in engineered tissues. In this Review, we consider different gradients present in natural tissues and discuss their critical importance in functional tissue engineering. Using this basis, we consolidate the existing fabrication methods into four categories: *additive manufacturing*, *component redistribution*, *controlled phase changes,* and *post-modification*. We have illustrated this with recent examples, highlighted prominent trends in the field, and outlined a set of criteria and perspectives for gradient fabrication.

Gradients in Biology

This Review provides a comprehensive overview of recent approaches to forming gradient biomaterials for tissue engineering. Gradients are continuous transitions in the magnitude of a property along an axis and are a pervasive feature of biology, with conserved functional roles in tissue development and physiology. Here, we consider five classes of gradients that are widely found in natural tissues and tissue interfaces. *Cellular gradients* involve transitions in the density of one or more cell types, for example, **osteochondral tissue (see Glossary)** exhibits depth-dependent differences from the articulating surface to the underlying bone, with graded densities of **chondrocytes**, **hypertrophic chondrocytes** and **osteoblasts** [1-3]. *Compositional gradients* are transitions in extracellular matrix (ECM) components, for example, mineral gradients are found in the dentin of human teeth [4], while collagen, proteoglycan, and hydration gradients are present throughout **articular cartilage** [5]. *Architectural gradients* are transitions in the organization of tissue components, such as the changes in porosity present in **cortical bone** [6] or the differences in fiber orientation across cardiac tissue [7]. Changes in tissue composition and architecture give rise to *mechanical gradients*, including transitions in compressive, tensile, and shear properties. Mechanical gradients are commonly found at load-bearing musculoskeletal interfaces, such as **entheses**, where they play an important role in the transmission of applied stresses [8].

Tissue gradients are established during development and maturation, processes that are guided by spatial variance in biochemical and biophysical cues [9]. In particular, *morphogen gradients* of

morphogens can arise through point-source diffusion or more complex intermediary mechanisms involving matrix components or extracellular vesicles [10]. These morphogen gradients generate cellular, compositional, architectural, and mechanical gradients by spatially regulating cell proliferation, migration, and differentiation [11]. For example, osteochondral tissue is derived from gradients of morphogens, such as Indian hedgehog, parathyroid hormone-related protein, and different bone morphogenetic proteins (BMPs) [12]. These morphogen gradients direct the differentiation of an initially homogeneous pool of **osteochondroprogenitors** into a gradient of mature cells comprising chondrocytes, hypertrophic chondrocytes, and osteoblasts. These different cell populations secrete distinct ECM components that provide the tissue with gradient mechanical properties to support the load-bearing function of osteochondral tissue [13].

Engineering Gradients *In Vitro*

These various gradients are often overlooked during *in vitro* tissue engineering. This omission is surprising given the importance of gradients to physiological function and the objective of tissue engineering: to replicate native tissue structures for *in vitro* modeling or *in vivo* tissue replacement [14]. Although homogenous tissue constructs can provide information pertaining to physiology or pathology, a lack of structural organization can mask or limit contributing factors or functional outputs. Similarly, while clinical benefit can be realized by using uniform tissue grafts, their simplicity can restrict graft integration and limit full functional restoration [15]. Accordingly, the development of new methods that enable more faithful recreation of natural morphologies has emerged as a

major focus of translational tissue engineering. While acknowledging that specialized culture systems can present soluble morphogen gradients *via* the cell media [16, 17], this Review focuses on the fabrication of gradient biomaterials for tissue engineering. Past reviews have focused on specific tissue gradients [18, 19] and specific gradient fabrication methods, such as 3D printing [20] microfluidics [21] electrospinning [22] self-assembly [22] and phase separation [22] In recent years, there have been a number of new methods and adapted approaches that have presented new opportunities for tissue engineering. Here, we discuss these recent developments as part of a broad and comprehensive overview of gradient biomaterial fabrication. We define four overarching strategies that can be employed to form gradients: additive manufacturing, component redistribution, controlled phase changes, and post-modification (**Figure 1, Key Figure**). We discuss key methods in each of these categories and explore their rationale, mechanism, benefits, and limitations. Finally, we outline a set of key criteria for those seeking to develop new fabrication methods for gradient tissue engineering.

Additive Manufacturing

An early additive manufacturing approach was the use of adhesives to bind two or more solid biomaterial layers. For instance, cellularized osteochondral scaffolds have been prepared by using a small amount of solvent glue to bind different polymeric scaffolds [23]. Glues such as alginate-boronic acid have been developed to bind pre-cast hydrogels, such as agarose, acrylamide, and chitosan-catechol [24]. In these cases, however, the attractive interactions within each material layer

are generally stronger than those bridging the interface, a situation that can result in delamination between the stacked layers. Thus, more recent work has focused on methods that can generate material layers without requiring an intermediary adhesive (**Figure 1A**). For example, the addition of a liquid precursor to a mold followed by partial crosslinking can be repeated to build up sequentially layered structures. This approach has recently been used by Guo and coworkers to create compositional gradients of mineralizing peptide in stacked silk fibroin hydrogels (**Figure 2A**) [25] and by Ko and coworkers to form compositional gradients in gelatin methacryloyl (GelMA) hydrogels [26]. Meanwhile, Parisi and coworkers showed that slurries of collagen and hydroxyapatite (HAP) at varying ratios could be sequentially stacked and collectively lyophilized to form integrated osteochondral scaffolds with compositional and mechanical gradients [27]. In 2016, Levingstone and coworkers reported an "iterative layering freeze-drying" approach employing multiple steps of **lyophilization**, crosslinking, and rehydration to create trilayer osteochondral scaffolds [28]. Meanwhile, an ingenious method reported by Wei and coworkers in 2017 showed that pre-cast hydrogel modules could be assembled into gradient biomaterials using a Schiff base “self-healing” mechanism [29]. An inherent limitation of all of these methods is that the material is composed of discrete layers (a stepped transition) rather than a smooth profile (a continuous gradient).

Greater structural complexity can be achieved using three-dimensional (3D) printing, in which a digital model is replicated as a solid or porous 3D object using controlled fluid deposition [20, 30, 31]. Mechanically-graded structures can be assembled by varying the ink composition or the print design.

In 2017, Trachtenberg and coworkers reported a gradient distribution of HAP nanoparticles in a 3D printed composite scaffold [32], while in 2019, Bittner and coworkers described the use of 3D fiber deposition to create poly(ε-caprolactone) (PCL)-based scaffolds with architectural gradients (porosity) and compositional gradients [33]. Meanwhile, 3D printed scaffolds with pore size gradients were reported by Di Luca and coworkers in 2016 and used to spatially modulate the **chondrogenic** differentiation [34] or **osteogenic** differentiation [35] of human **mesenchymal stem cells** (hMSCs). In 2020, Smith and coworkers also described the use of extrusion-based 3D printing to generate compositional and architectural (porosity) gradients to direct stem cell differentiation down the osteogenic lineage. The authors observed that increased concentration of β-tricalcium phosphate and higher scaffold porosity induced a more mature osteogenic phenotype [36]. Other groups have also recently used 3D printed scaffolds with graded pores as sacrificial templates [37, 38]. Although the majority of studies have reported the fabrication of vertical gradients, improvements in instrumentation have enabled the effective printing of lateral gradients. In 2019, Diaz-Gomez and coworkers described the use of multi-material segmented fiber printing to generate lateral gradients in composition and porosity [39], while in 2020, Giachini and coworkers used a feedback loop to synchronize extrusion and deposition to print multidirectional lateral gradients in composition, architecture, and stiffness [40].

These examples all focus on the fabrication of *acellular* gradient scaffolds, which can be seeded with cells after printing. An alternative strategy is 3D **bioprinting**, in which cells can be printed in either

biomaterial-free [41, 42] or biomaterial-based **bioinks** [43, 44]. High-energy processes, such as selective laser sintering, are poorly suited for printing viable cells, but extrusion printing, inkjet printing, and lithography-based printing can all be used to fabricate structures with high cell viability [45]. The inclusion of cells within the bioink presents the opportunity to directly fabricate defined cellular gradients. In 2017, Graham and coworkers generated different high-resolution tissue architectures by printing cell-laden droplets, including cellular gradients of osteoblasts and chondrocytes [46]. Meanwhile, in 2015, Hardin and coworkers demonstrated the use of microfluidic printheads to achieve controlled mixing of different inks before deposition, which allowed for continuous gradients to be formed in the extruded fibers [47]. In 2019, Idaszek and coworkers used this principle to mix doped alginate-based solutions for the bioprinting of graded cell-laden constructs to mimic the ECM organization of native cartilage (**Figure 2B**) [48]. In 2017, Liu and coworkers reported the use of a microfluidic mixing printhead with multiple input channels to controllably deposit up to seven inks and generate tunable structures with various cellular and compositional gradients [49]. The major benefit of 3D printing is the precise spatial control, which enables the generation of multiple gradients within tunable material architectures. However, only a small class of materials have the required characteristics needed for 3D printing, and only a subset of these are capable of supporting viable cell populations [50, 51].

Other continuous deposition processes can also be used to fabricate gradient materials. For example, commercially-available “gradient makers” continually feed solutions from different reservoirs into a

single joined outlet, with the mixed liquid then deposited and cast in a mold. By controlling the relative flow rates during the casting process, different gradients can be produced. In 2018, Zhu and coworkers used a gradient maker to generate mechanically-graded tissue constructs by casting a chondrocyte-laden hydrogel precursor solution with two biopolymer concentrations [52]. Controlled fluid deposition can also be achieved through the use of bespoke microfluidic platforms [53]. In 2017, Orsi and coworkers reported the fabrication of polyacrylamide hydrogels with mechanical gradients (stiffness) using a chamber integrated with multiple microfluidic inlets [54]. In 2019, Hubka and coworkers used a similar principle to form gradients of perlecan domain I across hyaluronic acid (HA)-based hydrogels. The perlecan domain was then used to sequester and release fibroblast growth factor; a morphogen gradient that was used to direct cell migration [55]. Two innovative approaches were reported in 2019, both employing microfluidic mixing and deposition. Xin and coworkers used microfluidic droplet generators to produce poly(ethylene glycol) (PEG)-based microgels, which were deposited into syringes and used to form microporous annealed particle hydrogels. By adjusting the input polymer components during the microdroplet fabrication, the authors produced hydrogels with gradients in microgel composition that were preserved post-annealing [56]. Meanwhile, Costantini and coworkers used an adjustable valve-based flow-focusing junction to generate foams with tunable bubble size. This method was used to fabricate gelatin and gelatin/HAP scaffolds with architectural gradients in pore size (80–800 μm) (**Figure 2C**) [57].

By controlling the fluid deposition process, **electrospinning** can also be used to fabricate gradient materials. Typically, reservoirs loaded with different polymer solutions are either sequentially deposited or mixed at varying ratios and then controllably electrospun onto a moving collector [58, 59]. In 2017, Kishan and coworkers reported the use of sequential electrospinning to generate meshes with compositional gradients of two different poly(ester urethane urea) fibers and architectural transitions in fiber alignment (**Figure 2D**) [60]. A similar approach was described by Khoo and coworkers in 2019, in which trilayer gelatin meshes were fabricated with architectural gradients in fiber diameter (227–679 nm) and pore size (1.14–4.93 μm^2) [61]. In 2019, Horner and coworkers reported an example of sequential core-shell electrospinning, in which the ratio between the PEG core and the PCL shell was varied during the deposition process. This method produced scaffolds with architectural gradients in fiber shell thickness and mechanical gradients in compressive modulus (3–19 kPa), thus allowing the effect of mechanical gradients upon hMSC differentiation to be studied in scaffolds with homogeneous composition and topography [62]. Overall, electrospinning, microfluidics, and gradient makers have enabled the rapid fabrication of continuously graded biomaterials, however, these methods are generally restricted to simple, unidirectional gradients.

Component Redistribution

The previous examples all involve the direct deposition of materials at different spatial co-ordinates along the gradient axis. An alternative approach is to start with a homogenous system and use an applied force to redistribute components into a gradient (**Figure 1B**). In 2020, Forget and coworkers

reported that vortex mixing could be used to redistribute dried sucrose microparticles by size, based on the principle of granular convection. The sucrose microparticles were used as porogens to template the formation of polyester-ether scaffolds with architectural gradients in pore size (**Figure 3A**) [63]. A more common strategy is the redistribution of fluid components through the use of controlled demixing processes. An early example of this approach is the use of centrifugal forces to fabricate collagen-glycosaminoglycan scaffolds with architectural gradients in pore size [64] and crosslinked PCL fibril scaffolds with architectural gradients (porosity) and morphogen gradients [65]. More recently, it has been shown that spontaneous demixing can be used for gradient biomaterial fabrication. Li and coworkers reported in 2019 that density differences between mixed fluid phases could lead to predictable demixing and the formation of materials bearing tunable compositional, mechanical, and morphogen gradients [66]. This method was used to present a gradient of BMP-2 across a GelMA hydrogel laden with hMSCs, in order to locally stimulate osteogenic differentiation and mineralization during osteochondral tissue engineering (**Figure 3B**). While the technology can support multiple gradient applications, the system requires a density difference and is restricted to a single gradient in one construct. An alternative approach is to use microfluidic devices to create controlled flow shear stretching and diffusion spreading, which was used in early work to fabricate compositional gradients [67]. More recently, thermally-induced convective flow has been used to form biomaterials bearing compositional gradients without the use of microfluidics. Canadas and coworkers reported in 2018 that composite gradient hydrogels could be prepared by mixing a cooled

solution of GelMA and gellan gum to a similar solution that had been pre-warmed and doped with HAP. A 10°C temperature difference between the two fluids was sufficient to generate compositional gradients in HAP, which were immobilized by gelation and used for osteochondral tissue engineering [17].

Convection, gravity or buoyancy-based approaches exploit physical material differences (*e.g.*, temperature, size, density), which enable gradients to be formed without needing to modify any of the components. Other approaches have sought to modify individual tissue engineering components so that they can be selectively manipulated using applied fields. In 2020, Zwi-Dantsis and coworkers used antibody-conjugated superparamagnetic iron oxide nanoparticles (SPIONs) to magnetize cardiomyocytes derived from human induced pluripotent stem cells. An external magnetic field was then used to generate different cellular gradients of cardiomyocytes, encapsulated in collagen hydrogels for cardiac tissue engineering [68]. A similar approach was reported by Li and coworkers in 2018, who showed that BMP-2 growth factor could be loaded into heparin-modified SPIONs and selectively redistributed into a gradient using an external magnetic field [69]. These morphogen gradients were formed across agarose hydrogels laden with hMSCs to form integrated osteochondral tissue constructs. Meanwhile, in 2020, Xu and coworkers formed biomaterials with compositional and mechanical gradients using electric field migration. In this work, β-sheet rich silk nanofibers moved to the anode of an applied electric field, with the migration kinetics tuned to the gelation rate

of the surrounding polymer (GelMA, *N*-isopropylacrylamide or amorphous silk nanofiber solution) (**Figure 3C**) [70].

Controlled Phase Changes

The examples discussed thus far have all involved the controlled distribution of materials. An alternative approach is to form gradients through spatially-controlled crosslinking, a particularly attractive option for fabricating materials with architectural or mechanical gradients (**Figure 1C**). Graded light exposure has been widely used to vary the degree of crosslinking across different hydrogels. Major and coworkers recently used gradient photomasks to produce GelMA hydrogels with continuous mechanical gradients in stiffness (5–38 kPa). The authors showed that adipose-derived stem cells encapsulated in low-stiffness regions exhibited an increased cellular and nuclear volume and enhanced nuclear localization of mechanosensitive proteins (**Figure 4A**) [71]. Meanwhile, Dou and coworkers used sliding photomasks to fabricate polyacrylamide hydrogels with longitudinal mechanical gradients in stiffness (1–40 kPa) capable of guiding **glioma cell** migration [72].

An alternative, thermal-based approach was demonstrated by Kim and coworkers in 2015, who used a unidirectional freezing process to create a transition in the crystallinity of poly(vinyl alcohol) (PVA) hydrogels. This was possible due to the unusual hydrogelation mechanism of PVA, in which ice crystals induce the formation of localized polymer crystallites that facilitate network crosslinking [73]. This methodology was later extended to semi-interpenetrating networks of PVA and HA, which

widened the stiffness range to 20–200 kPa. In 2018, Mirab and coworkers used a similar approach to fabricate lyophilized starch/PVA scaffolds with architectural gradients in pore width (80–292 μm) (**Figure 4B**). A citric acid crosslinker, osteoblasts, cellulose, and HAP were incorporated into the scaffolds, which were then used for bone tissue engineering [74]. Similar methods have been used to create ice fronts that move through a liquid precursor, initiate ice crystallization, and generate materials with spatial differences in material porosity. This ice-templating approach was used by Bai and coworkers in 2015 to fabricate HAP scaffolds with architectural gradients in channel width (4.5–8.1 μm) [75]. In 2017, Pawelec and coworkers used a similar method to template collagen-based hydrogels with architectural gradients in pore size (80–600 μm), a permeability range that was shown to affect the migration of seeded osteoblast-like cells [76].

Post-Modification

The previous examples have involved gradient formation *during* fabrication; a counter-strategy is the post-modification of pre-formed solids or hydrogels (**Figure 1D**). This approach has been most readily used to produce materials with compositional gradients. Early examples involved the gradual introduction of solution components to scaffolds by dip-coating [77] or controlled immersion [78]. A more recent trend has been the use of controlled diffusion to generate uneven distributions of molecular components. In 2015, Gunnewiek and coworkers used molecular diffusion to create longitudinal and radial gradients of immoblized proteins across porous PCL scaffolds [79]. In 2018, Xu and coworkers reported that diffusion could be used to form gradients of a bifunctional crosslinker

across pre-cast Matrigel. The crosslinker was immobilized to the Matrigel, uncaged by light, and used as a reactive base to bind a semaphorin 3A (Sema3A), which was also introduced *via* a diffusion gradient (**Figure 5A**). Depth-dependent gradients of Sema3A are believed to direct radial migration of neurons during cortical development and the authors observed evidence of enhanced cortical regeneration after implanting the Sema3A Matrigel gradient into a rat model of traumatic brain injury [80]. Strategies based on controlled adsorption or diffusion are relatively simple and accessible, however, they often require an optimized set of parameters that limit the rate of a molecular process without impeding it entirely.

Post-modification can also be performed using spatially-modulated light exposure [81]. In 2016, Tong and coworkers reported the use of sliding photomasks to vary the photocrosslinking of norbornene-functionalized PEG hydrogels with cysteine-terminated RGD peptide. This method was applied to hydrogels that were already cast with a mechanical stiffness gradient [82]. Orthogonal compositional gradients were also reported by Vega and coworkers, who used sequential sliding photomasks to immobilize different peptides to norbornene-functionalized HA-based hydrogels (**Figure 5B**) [83]. An alternative approach was demonstrated in a seminal paper by Mosiewicz and coworkers in 2013. The authors showed that laser-scanning lithography could be used to uncage enzymatic peptide substrates tethered to PEG-based hydrogels. The resulting enzymatic crosslinking enabled the presentation of gradients of covalently-bound proteins, such as vascular endothelial growth factor [84]. Similar methods have been developed by the Shoichet group, in which light was used to

deprotect or uncage hydrogel-bound thiols that were used to subsequently bind bioactive peptides or proteins [85, 86]. In 2018, they showed that HA-based hydrogels functionalized with nitrodibenzofuran-caged thiols could form exposed thiol gradients following repeated two-photon laser scanning. An intermediary click reaction between the uncaged thiol and maleimide-functionalized streptavidin produced gradients of biotinylated epidermal growth factor, which was shown to direct cancer cell invasion [86].

General Criteria for Gradient Fabrication

The approaches discussed in this Review each have specific merits and limitations (**Table 1**). Taking these into consideration, several principles should be applied when designing a fabrication strategy for gradient tissue engineering. The first criterion is *the recreation of biologically-relevant profiles*. Stepped transitions commonly formed by sequential layering methods may be appropriate in certain tissue engineering scenarios, such as the bone-cartilage interface in osteochondral tissue. However, continuous transitions bear greater relevance to most physiological systems, enabling improved load transmission and avoiding interfaces that can present mechanical instability or exclude cells. This is linked with the second criterion: *the ability to generate complex gradients*. Many strategies, such as those employing gravity or buoyancy, are limited to the formation of single, linear gradients. In contrast, biological systems frequently exhibit gradients along different biological axes (*e.g.*, dorsoventral and anteroposterior patterning in the **neural tube** [87]) or in a nonlinear configuration (*e.g.*, radial transitions in the walls of blood vessels [88]). These systems may benefit from the greater

design flexibility offered by methods such as 3D printing or the combination of techniques, such as the formation of dual gradients using post-modification of photopatterned hydrogels [82]. Other convergent approaches could be envisaged, for example, by generating ice-templated PVA gradients during 3D printing, or by forming dual gradients by sequential magnetic field attraction and graded photocrosslinking. A third criterion is *the ability to generate dynamic gradients*. Natural systems exhibit dynamic changes in morphogen gradient profiles, most notably during different stages of development. This is a major challenge for biomaterial-based strategies, which is generally restricted to simple slow-release morphogen gradients. Cell-secreted enzymes have been used to degrade materials in response to phenotypic changes [89] and similar methods could be used to release morphogen gradients in tune with tissue development and maturation. Alternatively, DeForest and coworkers demonstrated photoreversible tethering of biomolecules to hydrogels, which could be used to extrinsically release morphogen gradients [90].

As well as these technical criteria, it is also important to consider factors that determine academic adoption and translational potential. In this regard, a fourth criterion is *the use of accessible equipment*. Widespread protocol adoption can be stifled by the specialist knowledge and high costs associated with certain techniques (*e.g.*, bioprinting, microfluidics, two-photon laser scanning). Greater accessibility can be achieved through the use of standard laboratory equipment (*e.g.*, centrifuges), the publication of detailed protocol papers, and the commercialization of dedicated technologies (*e.g.*, gradient makers). A related fifth criterion is *system versatility*. Many gradient

fabrication “platforms” are demonstrated using a single material, molecule, or tissue, however, techniques that can be widely applied to different systems can address the needs of a broader user base. In this regard, gradient fabrication should ideally not be constrained by a particular material property (*e.g.*, photoresponsivity, viscosity, magnetism). A sixth criterion, particularly important for translation, is *the system reproducibility and robustness*. Any scientific method should be reproducible under the reported conditions, however, it is also important that gradient fabrication is not restricted to a narrow parameter space. Ideally, standardized protocols should be used for fabrication with critical-to-quality attributes used to assess the tolerance of the system to process changes. This is linked with the last criterion: *the system scalability and throughput*. A key process change that should always be assessed is scaling: is the chosen fabrication platform capable of large-scale production of gradient materials? In this regard, systems that are highly automated, rapid, and reproducible will generally enable the high throughput manufacture required for translational applications.

Concluding Remarks

The tissue engineering community is fully focused on developing methods that can recreate the sophisticated architecture of natural tissues. Here, we have outlined methods for fabricating different gradients present in physiological systems: cellular, compositional, architectural, mechanical, and morphogen. We have presented a new categorization system for the four different gradient fabrication strategies based on their underlying rationale: additive manufacturing,

component redistribution, controlled phase changes, and post-modification. Many of the studies presented in this Review have focused on osteochondral tissue engineering, but we have also presented examples in which gradient biomaterials are used for *in vitro* bone and cardiac tissue engineering, and *in vivo* neural regeneration. These different approaches should be selected and adapted after considering the specific requirements of the target tissue and application. New methodologies are continually being pioneered, and to this end, we propose a set of ideal criteria for gradient fabrication: the recreation of biologically-relevant profiles, the ability to generate complex gradients, the use of widely-accessible equipment, the system versatility and the system reproducibility and robustness (**see Outstanding Questions**). We hope that this Review will aid and inspire those seeking to develop new gradient biomaterial fabrication methods as well as those applying existing techniques to engineer gradient tissues.

Acknowledgments

C.L. was supported by a Top University Strategic Alliance PhD Scholarship from Taiwan. J.P.K.A. acknowledges support from the Medical Research Council (MRC) (MR/S00551X/1). The authors thank Li Li for the schematic drawing of the Key Figure. L.O. and M.M.S. acknowledge the financial support from Engineering and Physical Sciences Research Council (EPSRC) Programme Grant "Engineering growth factor microenvironments - a new therapeutic paradigm for regenerative medicine" (EP/P001114/1). M.M.S. acknowledges support from the grant from the UK Regenerative Medicine Platform "Acellular / Smart Materials – 3D Architecture" (MR/R015651/1).

Glossary

Articular cartilage: Load-bearing collagenous tissue present at the end of long bones.

Bioink: The fluid, typically containing viable cells, that is deposited during bioprinting.

Bioprinting: The use of computer-aided transfer processes for the patterning and assembly of living and nonliving materials with a defined 2D or 3D architecture.

Cortical bone: Dense mineralized tissue found predominantly at the surface of long bones and flat bones.

Chondrocytes: Mononucleate, rounded cells of mesenchymal origin that are responsible for the formation and remodeling of cartilage tissue.

Chondrogenic: Relating to the formation of bone.

Electrospinning: A processing method that uses electric fields to generate fibrous scaffolds from polymer solutions.

Entheses: Interfacial tissue where bone forms a connection to a tendon, ligament, fascia, or capsule.

Glioma cell: A cancer cell type thought to arise from nonmalignant glial cells.

Hypertrophic chondrocytes: Non-proliferative swollen chondrocytes that direct mineralization and vascularization during endochondral bone formation.

Lyophilization: The sublimation of ice from frozen materials at reduced pressure, synonym for freeze-drying.

Mesenchymal stem cell: Multipotent cells that give rise to cells of chondrogenic, osteogenic, and adipogenic lineage.

Neural tube: The embryonic precursor to the central nervous system.

Osteoblasts: Mononucleate, cuboid cells of mesenchymal origin that are responsible for the formation of bone tissue.

Osteochondral tissue: Interfacial tissue comprising subchondral bone and articular cartilage.

Osteochondroprogenitors: Progenitor cells of mesenchymal origin that give rise to osteoblasts or chondrocytes.

Osteogenic: Relating to the formation of bone.

References

1. Sophia Fox, A.J. Et Al. (2009) The Basic Science Of Articular Cartilage: Structure, Composition, And Function. Sports Health 1 (6), 461-468.

2. Ren, X. Et Al. (2016) Engineering Zonal Cartilage Through Bioprinting Collagen Type II Hydrogel Constructs With Biomimetic Chondrocyte Density Gradient. BMC Musculoskelet Disord 17, 301.

3. Jadin, K.D. Et Al. (2005) Depth-Varying Density And Organization Of Chondrocytes In Immature And Mature Bovine Articular Cartilage Assessed By 3D Imaging And Analysis. J Histochem Cytochem 53 (9), 1109-1119.

4. Djomehri, S.I. Et Al. (2015) Mineral Density Volume Gradients In Normal And Diseased Human Tissues. Plos One 10 (4), E0121611.

5. Bergholt, M.S. Et Al. (2016) Raman Spectroscopy Reveals New Insights Into The Zonal Organization Of Native And Tissue-Engineered Articular Cartilage. ACS Cent Sci 2 (12), 885-895.

6. Baron, C. (2012) Using The Gradient Of Human Cortical Bone Properties To Determine Age-Related Bone Changes Via Ultrasonic Guided Waves. Ultrasound Med Biol 38 (6), 972-981.

7. Tobon, C. Et Al. (2013) A Three-Dimensional Human Atrial Model With Fiber Orientation. Electrograms And Arrhythmic Activation Patterns Relationship. Plos One 8 (2), e50883.

8. Thomopoulos, S. Et Al. (2003) Variation Of Biomechanical, Structural, And Compositional Properties Along The Tendon To Bone Insertion Site. J Orthopaedic Res 21 (3), 413-419.

9. Zhu, M. Et Al. (2020) Spatial Mapping Of Tissue Properties In Vivo Reveals A 3D Stiffness Gradient In The Mouse Limb Bud. Proc Natl Acad Sci U S A 117 (9), 4781-4791.

10. Zhu, A.J. And Scott, M.P. (2004) Incredible Journey: How Do Developmental Signals Travel Through Tissue? Genes Dev 18 (24), 2985-2997.

11. Christian, J.L. (2012) Morphogen Gradients In Development: From Form To Function. Wiley Interdiscip Rev Dev Biol 1 (1), 3-15.

12. Di Luca, A. Et Al. (2015) The Osteochondral Interface As A Gradient Tissue: From Development To The Fabrication Of Gradient Scaffolds For Regenerative Medicine. Birth Defects Research. Part C, Embryo Today : Reviews 105 (1), 34-52.

13. Kronenberg, H.M. (2003) Developmental Regulation Of The Growth Plate. Nature 423 (6937), 332-336.

14. Armstrong, J.P.K. And Stevens, M.M. (2019) Emerging Technologies For Tissue Engineering: From Gene Editing To Personalized Medicine. Tissue Eng Part A 25 (9-10), 688-692.

15. Armstrong, J.P.K. And Stevens, M.M. (2020) Using Remote Fields For Complex Tissue Engineering. Trends Biotechnol 38 (3), 254-263.

16. Iannucci, L.E. Et Al. (2019) Cellular And Chemical Gradients To Engineer The Meniscus-To-Bone Insertion. Adv Healthc Mater 8 (7), e1800806.

17. Canadas, R.F. Et Al. (2018) Biochemical Gradients To Generate 3D Heterotypic-Like Tissues With Isotropic And Anisotropic Architectures. Adv Funct Mater 28 (48), e1804148

18. Ansari, S. Et Al. (2019) Engineering Of Gradient Osteochondral Tissue: From Nature To Lab. Acta Biomater 87, 41-54.

19. Calejo, I. Et Al. (2020) A Physiology-Inspired Multifactorial Toolbox In Soft-To-Hard Musculoskeletal Interface Tissue Engineering. Trends Biotechnol 38 (1), 83-98.

20. Bracaglia, L.G. Et Al. (2017) 3D Printing For The Design And Fabrication Of Polymer-Based Gradient Scaffolds. Acta Biomater 56, 3-13.

21. Wang, X. Et Al. (2017) Concentration Gradient Generation Methods Based On Microfluidic Systems. RSC Advances 7 (48), 29966-29984.

22. Seidi, A. Et Al. (2013) Gradient Nanofiber Scaffolds For Tissue Engineering. J Nanosci Nanotechnol 13 (7), 4647-4655.

23. Niederauer, G.G. Et Al. (2000) Evaluation Of Multiphase Implants For Repair Of Focal Osteochondral Defects In Goats. Biomaterials 21 (24), 2561-2574.

24. Hong, S.H. Et Al. (2019) Alginate-Boronic Acid: Ph-Triggered Bioinspired Glue For Hydrogel Assembly. Adv Funct Mater. e1908497

25. Guo, J. Et Al. (2017) Multiscale Design And Synthesis Of Biomimetic Gradient Protein/Biosilica Composites For Interfacial Tissue Engineering. Biomaterials 145, 44-55.

26. Ko, H. Et Al. (2019) A Simple Layer-Stacking Technique To Generate Biomolecular And Mechanical Gradients In Photocrosslinkable Hydrogels. Biofabrication 11 (2), 025014.

27. Parisi, C. Et Al. (2020) Biomimetic Gradient Scaffold Of Collagen-Hydroxyapatite For Osteochondral Regeneration. J Tissue Eng 11, 204173141989606.

28. Levingstone, T.J. Et Al. (2016) Multi-Layered Collagen-Based Scaffolds For Osteochondral Defect Repair In Rabbits. Acta Biomater 32, 149-160.

29. Wei, Z. Et Al. (2017) Dual Cross-Linked Biofunctional And Self-Healing Networks To Generate User-Defined Modular Gradient Hydrogel Constructs. Adv Healthc Mater 6 (16), e1700523.

30. Ouyang, L. Et Al. (2020) Assembling Living Building Blocks To Engineer Complex Tissues. Adv Funct Mater. e1909009.

31. Ouyang, L. Et Al. (2019) Void-Free 3D Bioprinting For In Situ Endothelialization And Microfluidic Perfusion. Adv Funct Mater 30 (1), e1908349.

32. Trachtenberg, J.E. Et Al. (2017) Extrusion-Based 3D Printing Of Poly(Propylene Fumarate) Scaffolds With Hydroxyapatite Gradients. J Biomater Sci Polym Ed 28 (6), 532-554.

33. Bittner, S.M. Et Al. (2019) Fabrication And Mechanical Characterization Of 3D Printed Vertical Uniform And Gradient Scaffolds For Bone And Osteochondral Tissue Engineering. Acta Biomater 90, 37-48.

34. Di Luca, A. Et Al. (2016) Influencing Chondrogenic Differentiation Of Human Mesenchymal Stromal Cells In Scaffolds Displaying A Structural Gradient In Pore Size. Acta Biomater 36, 210-219.

35. Di Luca, A. Et Al. (2016) Gradients In Pore Size Enhance The Osteogenic Differentiation Of Human Mesenchymal Stromal Cells In Three-Dimensional Scaffolds. Sci Rep 6, 22898.

36. Smith, B.T. Et Al. (2019) Multimaterial Dual Gradient Three-Dimensional Printing For Osteogenic Differentiation And Spatial Segregation. Tissue Eng Part A 26 (5-6), 239-252.

37. Montazerian, H. Et Al. (2019) Permeability And Mechanical Properties Of Gradient Porous PDMS Scaffolds Fabricated By 3D-Printed Sacrificial Templates Designed With Minimal Surfaces. Acta Biomater 96, 149-160.

38. Nowicki, M.A. Et Al. (2016) 3D Printing Of Novel Osteochondral Scaffolds With Graded Microstructure. Nanotechnology 27 (41), 414001.

39. Diaz-Gomez, L. Et Al. (2019) Three-Dimensional Printing Of Tissue Engineering Scaffolds With Horizontal Pore And Composition Gradients. Tissue Eng Part C Methods 25 (7), 411-420.

40. Giachini, P. Et Al. (2020) Additive Manufacturing Of Cellulose-Based Materials With Continuous, Multidirectional Stiffness Gradients. Sci Adv 6 (8), eaay0929.

41. Ayan, B. Et Al. (2020) Aspiration-Assisted Bioprinting For Precise Positioning Of Biologics. Sci Adv 6 (10), eaaw5111.

42. Jeon, O. Et Al. (2019) Individual Cell-Only Bioink And Photocurable Supporting Medium For 3D Printing And Generation Of Engineered Tissues With Complex Geometries. Materials Horizons 6 (8), 1625-1631.

43. Lee, A. Et Al. (2019) 3D Bioprinting Of Collagen To Rebuild Components Of The Human Heart. Science 365 (6452), 482-487.

44. Armstrong, J.P. Et Al. (2016) 3D Bioprinting Using A Templated Porous Bioink. Adv Healthc Mater 5 (14), 1724-1730.

45. Moroni, L. Et Al. (2018) Biofabrication Strategies For 3D In Vitro Models And Regenerative Medicine. Nat Rev Mater 3 (5), 21-37.

46. Graham, A.D. Et Al. (2017) High-Resolution Patterned Cellular Constructs By Droplet-Based 3D Printing. Sci Rep 7 (1), 7004.

47. Hardin, J.O. Et Al. (2015) Microfluidic Printheads For Multimaterial 3D Printing Of Viscoelastic Inks. Adv Mater 27 (21), 3279-3284.

48. Idaszek, J. Et Al. (2019) 3D Bioprinting Of Hydrogel Constructs With Cell And Material Gradients For The Regeneration Of Full-Thickness Chondral Defect Using A Microfluidic Printing Head. Biofabrication 11 (4), 044101.

49. Liu, W. Et Al. (2017) Rapid Continuous Multimaterial Extrusion Bioprinting. Adv Mater 29 (3). e1604630.

50. Ouyang, L. Et Al. (2016) 3D Printing Of Shear-Thinning Hyaluronic Acid Hydrogels With Secondary Cross-Linking. ACS Biomater Sci Eng 2 (10), 1743-1751.

51. Ouyang, L. Et Al. (2017) A Generalizable Strategy For The 3D Bioprinting Of Hydrogels From Nonviscous Photo-Crosslinkable Inks. Adv Mater 29 (8), 1604983.

52. Zhu, D.Q. Et Al. (2018) Mimicking Cartilage Tissue Zonal Organization By Engineering Tissue-Scale Gradient Hydrogels As 3D Cell Niche. Tissue Eng Part A 24 (1-2), 1-10.

53. Burdick, J.A. Et Al. (2004) Fabrication Of Gradient Hydrogels Using A Microfluidics/Photopolymerization Process. Langmuir 20 (13), 5153-5156.

54. Orsi, G. Et Al. (2017) A New 3D Concentration Gradient Maker And Its Application In Building Hydrogels With A 3D Stiffness Gradient. J Tissue Eng Regen Med 11 (1), 256-264.

55. Hubka, K.M. Et Al. (2019) Perlecan Domain I Gradients Establish Stable Biomimetic Heparin Binding Growth Factor Gradients For Cell Migration In Hydrogels. Acta Biomater 97, 385-398.

56. Xin, S.J. Et Al. (2019) Creating Physicochemical Gradients In Modular Microporous Annealed Particle Hydrogels Via A Microfluidic Method. Adv Funct Mater 30 (6), e1907102.

57. Costantini, M. Et Al. (2019) 3D-Printing Of Functionally Graded Porous Materials Using On-Demand Reconfigurable Microfluidics. Angew Chem Int Ed Engl 58 (23), 7620-7625.

58. Zhang, X. Et Al. (2012) Flexible Generation Of Gradient Electrospinning Nanofibers Using A Microfluidic Assisted Approach. Langmuir 28 (26), 10026-10032.

59. Chow, L.W. Et Al. (2014) Peptide-Directed Spatial Organization Of Biomolecules In Dynamic Gradient Scaffolds. Adv Healthc Mater 3 (9), 1381-1386.

60. Kishan, A.P. Et Al. (2017) Fabrication Of Macromolecular Gradients In Aligned Fiber Scaffolds Using A Combination Of In-Line Blending And Air-Gap Electrospinning. Acta Biomater 56, 118-128.

61. Khoo, W. Et Al. (2019) Fracture Behavior Of Multilayer Fibrous Scaffolds Featuring Microstructural Gradients. Materials & Design 184, 108184.

62. Horner, C.B. Et Al. (2019) Spatially Regulated Multiphenotypic Differentiation Of Stem Cells In 3D Via Engineered Mechanical Gradient. ACS Appl Mater Interfaces 11 (49), 45479-45488.

63. Forget, A. Et Al. (2020) Facile Preparation Of Tissue Engineering Scaffolds With Pore Size Gradients Using The Muesli Effect And Their Application To Cell Spheroid Encapsulation. J Biomed Mater Res B Appl Biomater.

64. Harley, B.A. Et Al. (2006) Fabricating Tubular Scaffolds With A Radial Pore Size Gradient By A Spinning Technique. Biomaterials 27 (6), 866-874.

65. Oh, S.H. Et Al. (2011) Creating Growth Factor Gradients In Three Dimensional Porous Matrix By Centrifugation And Surface Immobilization. Biomaterials 32 (32), 8254-8260.

66. Li, C. Et Al. (2019) Buoyancy-Driven Gradients For Biomaterial Fabrication And Tissue Engineering. Adv Mater 31 (17), e1900291.

67. He, J. Et Al. (2010) Rapid Generation Of Biologically Relevant Hydrogels Containing Long-Range Chemical Gradients. Adv Funct Mater 20 (1), 131-137.

68. Zwi-Dantsis, L. Et Al. (2020) Remote Magnetic Nanoparticle Manipulation Enables The Dynamic Patterning Of Cardiac Tissues. Adv Mater 32 (6), e1904598.

69. Li, C. Et Al. (2018) Glycosylated Superparamagnetic Nanoparticle Gradients For Osteochondral Tissue Engineering. Biomaterials 176, 24-33.

70. Xu, G. Et Al. (2020) Electric Field-Driven Building Blocks For Introducing Multiple Gradients To Hydrogels. Protein Cell. 11 (4), 267-285.

71. Major, L.G. Et Al. (2019) Volume Adaptation Controls Stem Cell Mechanotransduction. ACS Appl Mater Interfaces 11 (49), 45520-45530.

72. Dou, J. Et Al. (2020) Combination Stiffness Gradient With Chemical Stimulation Directs Glioma Cell Migration On A Microfluidic Chip. Anal Chem 92 (1), 892-898.

73. Kim, T.H. Et Al. (2015) Creating Stiffness Gradient Polyvinyl Alcohol Hydrogel Using A Simple Gradual Freezing-Thawing Method To Investigate Stem Cell Differentiation Behaviors. Biomaterials 40, 51-60.

74. Mirab, F. Et Al. (2018) Fabrication And Characterization Of A Starch-Based Nanocomposite Scaffold With Highly Porous And Gradient Structure For Bone Tissue Engineering. Biomedical Physics & Engineering Express 4 (5), 055021.

75. Bai, H. Et Al. (2015) Biomimetic Gradient Scaffold From Ice-Templating For Self-Seeding Of Cells With Capillary Effect. Acta Biomater 20, 113-119.

76. Pawelec, K.M. Et Al. (2017) Ice-Templating Of Anisotropic Structures With High Permeability. Mater Sci Eng C Mater Biol Appl 76, 628-636.

77. Phillips, J.E. Et Al. (2008) Engineering Graded Tissue Interfaces. Proc Natl Acad Sci U S A 105 (34), 12170-12175.

78. Liu, W. Et Al. (2014) Nanofiber Scaffolds With Gradients In Mineral Content For Spatial Control Of Osteogenesis. ACS Appl Mater Interfaces 6 (4), 2842-2849.

79. Gunnewiek, M.K. Et Al. (2015) Creeping Proteins In Microporous Structures: Polymer Brush-Assisted Fabrication Of 3D Gradients For Tissue Engineering. Adv Healthc Mater 4 (8), 1169-1174.

80. Xu, Z. Et Al. (2018) Regeneration Of Cortical Tissue From Brain Injury By Implantation Of Defined Molecular Gradient Of Semaphorin 3A. Biomaterials 157, 125-135.

81. Khetan, S. And Burdick, J.A. (2011) Patterning Hydrogels In Three Dimensions Towards Controlling Cellular Interactions. Soft Matter 7 (3), 830-838.

82. Tong, X.M. Et Al. (2016) Hydrogels With Dual Gradients Of Mechanical And Biochemical Cues For Deciphering Cell-Niche Interactions. Acs Biomater Sci Eng 2 (5), 845-852.

83. Vega, S.L. Et Al. (2018) Combinatorial Hydrogels With Biochemical Gradients For Screening 3D Cellular Microenvironments. Nat Commun 9 (1), 614.

84. Mosiewicz, K.A. Et Al. (2013) In Situ Cell Manipulation Through Enzymatic Hydrogel Photopatterning. Nat Mater 12 (11), 1072-1078.

85. Tam, R.Y. Et Al. (2017) Engineering Cellular Microenvironments With Photo- And Enzymatically Responsive Hydrogels: Toward Biomimetic 3D Cell Culture Models. Acc Chem Res 50 (4), 703-713.

86. Fisher, S.A. Et Al. (2018) Photo-Immobilized EGF Chemical Gradients Differentially Impact Breast Cancer Cell Invasion And Drug Response In Defined 3D Hydrogels. Biomaterials 178, 751-766.

87. Ulloa, F. And Briscoe, J. (2007) Morphogens And The Control Of Cell Proliferation And Patterning In The Spinal Cord. Cell Cycle 6 (21), 2640-2649.

88. Galliger, Z. Et Al. (2019) 3D Bioprinting For Lungs And Hollow Organs. Transl Res 211, 19-34.

89. Parmar, P.A. Et Al. (2016) Temporally Degradable Collagen-Mimetic Hydrogels Tuned To Chondrogenesis Of Human Mesenchymal Stem Cells. Biomaterials 99, 56-71.

90. Deforest, C.A. And Tirrell, D.A. (2015) A Photoreversible Protein-Patterning Approach For Guiding Stem Cell Fate In Three-Dimensional Gels. Nat Mater 14 (5), 523-531.

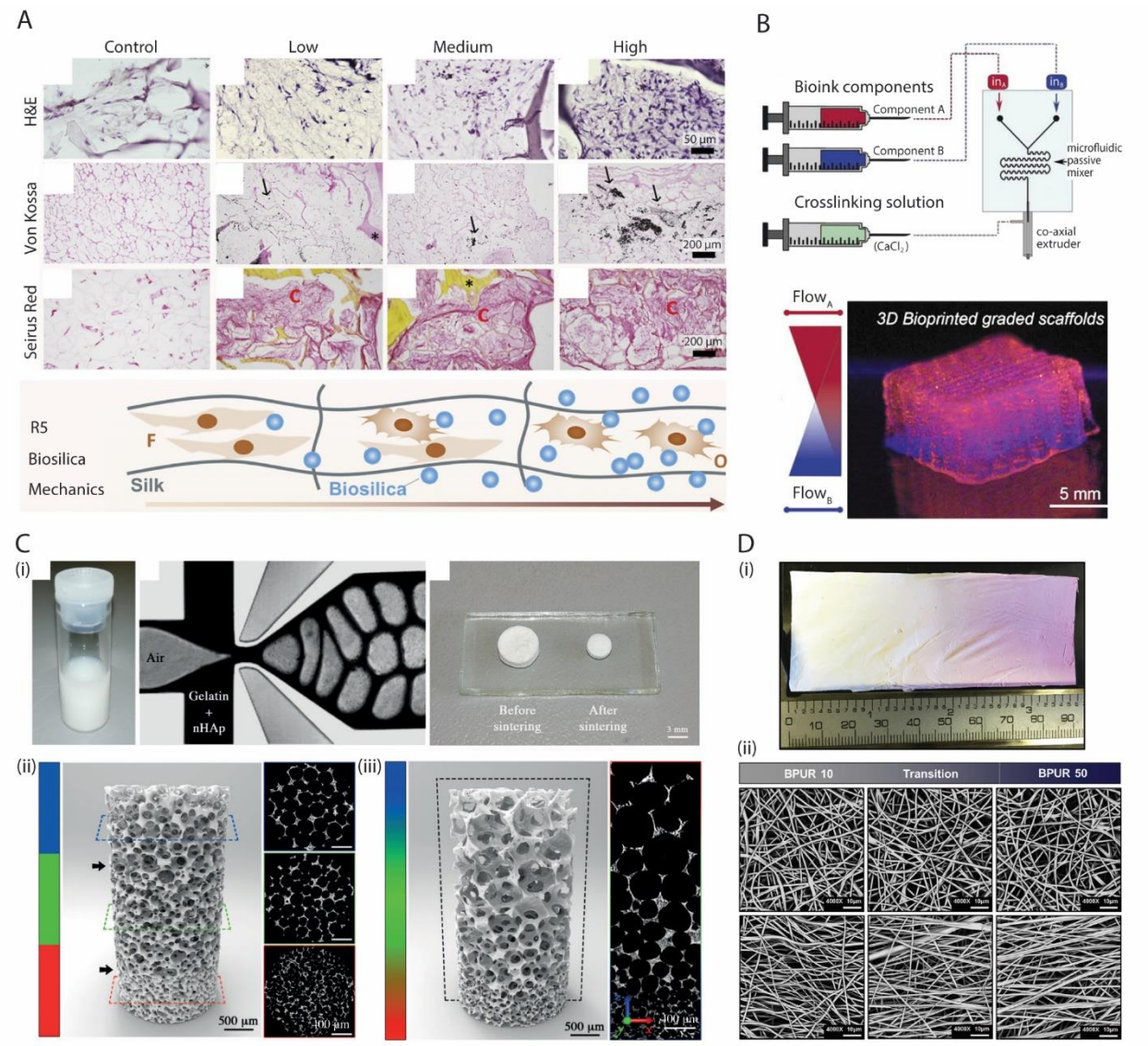
A
Control
Low
Medium
High
H&E
Von Kossa
Seirus Red
50 µm
200 µm
200 µm
C
C
C
R5
Biosilica
Mechanics
F
O
Silk
Biosilica
B
Bioink components
Component A
Component B
Crosslinking solution
(CaCl2)
microfluidic passive mixer
co-axial extruder
FlowA
FlowB
3D Bioprinted graded scaffolds
5 mm
C
(i)
Air
Gelatin + nHAp
Before sintering
After sintering
3 mm
(ii)
500 µm
500 µm
(iii)
500 µm
500 µm
D
(i)
(ii)
BPUR 10
Transition
BPUR 50

1

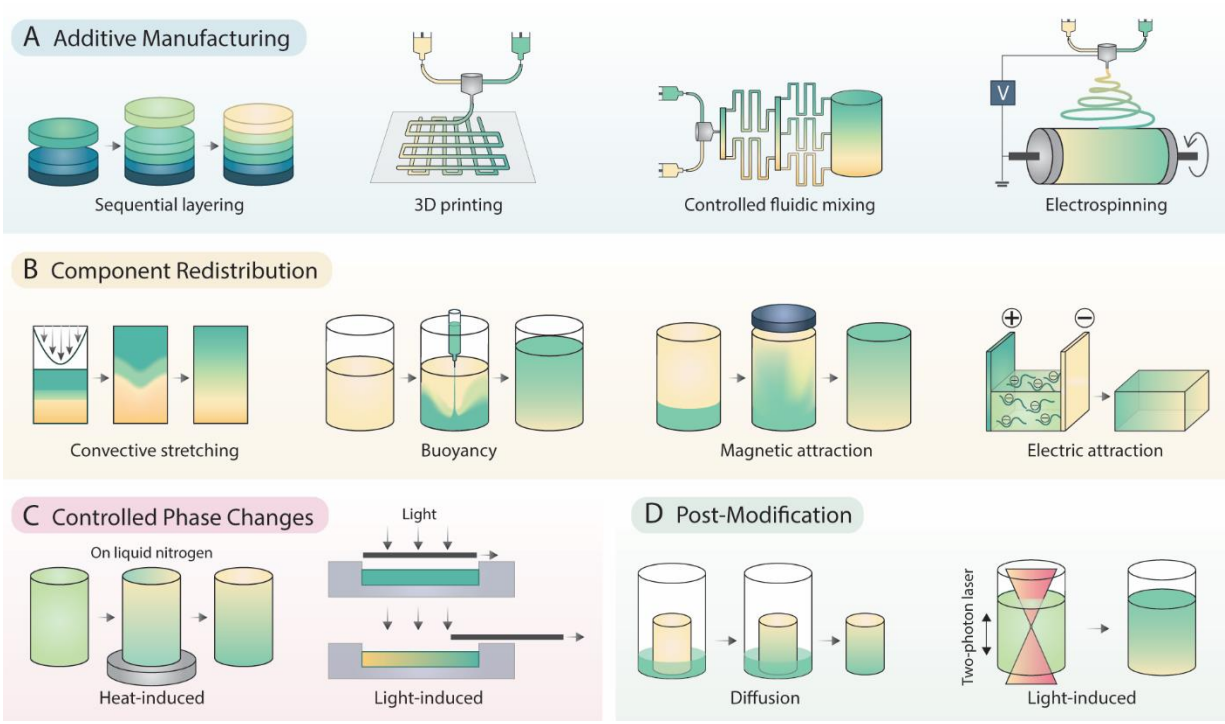

Figure 1. Four categories of gradient fabrication. (A) Additive manufacturing is an intuitive approach to gradient fabrication, with methods including sequential layering, 3D printing, controlled fluidic mixing, and electrospinning. (B) Component redistribution approaches produce gradients from an initially homogeneous distribution, for example, using convective stretching, buoyancy, magnetic fields or electric fields. (C) Controlled phase changes can also result in the formation of gradients from homogenous starting materials, typically using graded exposure to heat or light. (D) Post-modification involves the presentation of a gradient onto pre-formed materials, typically achieved by controlled component diffusion or photopatterning.

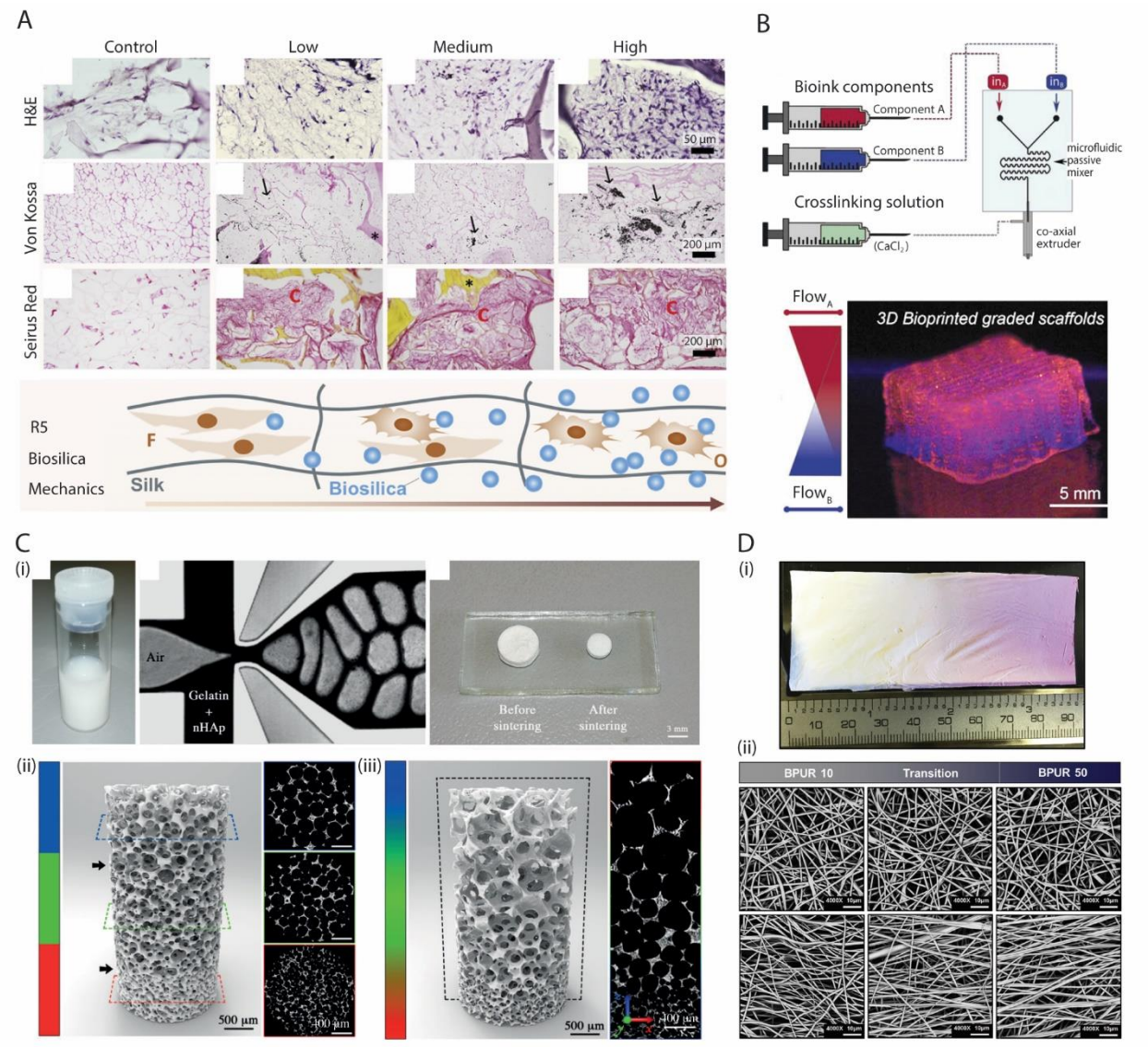

Figure 2. Additive manufacturing of gradient biomaterials. (A) Osteochondral tissue, engineered using mesenchymal stem cells seeded on a sequentially-layered scaffold with low, medium, and high loadings of a mineralizing peptide (R5). Reproduced with permission from [25]. (B) 3D printing gradient scaffolds using a microfluidic printing head to controllably mix solution components prior to extrusion. Reproduced with permission from [48]. (C) (i) Fabrication of scaffolds with gradient

porosity using a valve-based, flow-focusing microfluidic device to create gelatin/HAP foams with tunable bubble size. 3D reconstructions using micro computed tomography of the resulting (ii) multilayered and (iii) graded porous materials. Reproduced with permission from [57]. (D) (i) Gradient electrospun scaffolds fabricated from two different poly(ester urethane urea) fibers. (ii) Scanning electron micrographs of different regions across random and aligned gradient scaffolds. Reproduced with permission from [60].

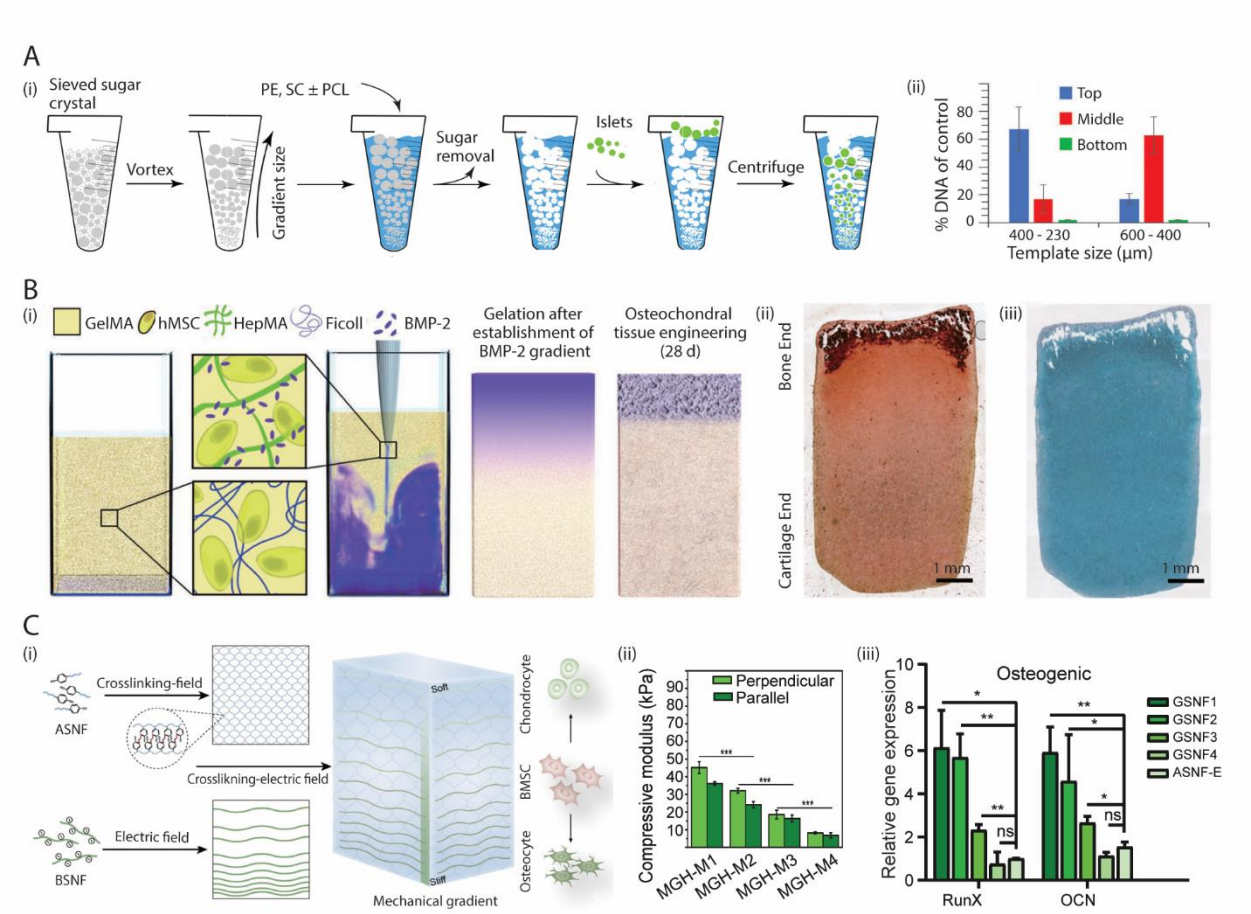

Figure 3. Component redistribution approaches for gradient biomaterial fabrication. (A) (i) Fabrication of scaffolds with pore size transitions templated by gradients of sugar particles (grey) formed *via* granular convection. After adding and crosslinking a polymer precursor solution (blue), the templates were dissolved and human pancreatic islets (green) were seeded in the resulting pores. (ii) The number of human islets retained throughout the scaffold with the different porogen size ranges. Reproduced with permission from [63]. (B) (i) Osteochondral tissue, engineered using hMSC-laden GelMA hydrogels, with buoyancy used to form a gradient of BMP-2 complexed with heparin methacrylate (HepMA). The resulting tissue was stained with (ii) Alizarin Red S to reveal the presence

of a mineralized cap and (iii) Alcian Blue staining to visualize the distribution of sulfated glycosaminoglycans. Reproduced with permission from [66]. (C) (i) Cell-supportive gradient biomaterials generated by the migration of silk nanofibers through hydrogel precursors under an applied electric field. (ii) Mechanical testing of silk-laden GelMA-based hydrogels showing a transition in compressive modulus. (iii) Gene expression of mesenchymal stem cells in different regions of the gradient hydrogels after 28 d of osteogenic differentiation. Reproduced with permission from [70].

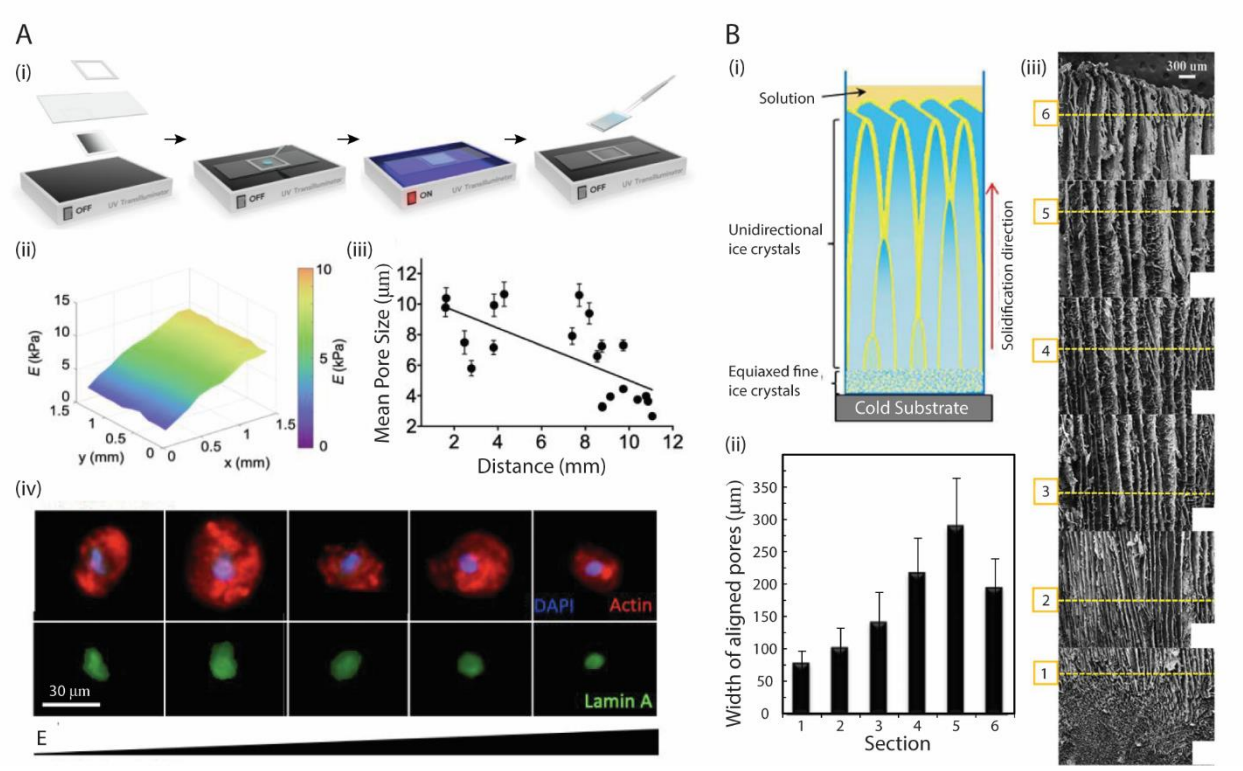

Figure 4. Controlled phase changes for gradient biomaterial fabrication. (A) (i) Fabrication of graded photo-crosslinkable biomaterials using gradient photomasks. (ii) Optical coherence elastography and (iii) pore size measurements were performed on the resulting materials to measure mechanical gradients (stiffness) and architectural gradients (porosity), respectively. (iv) Morphology of adipose-derived stem cells encapsulated in gradient GelMA hydrogels. Reproduced with permission from [71]. (B) (i) Scaffolds fabricated by ice-templating starch/PVA hydrogels under thermal gradients. (ii) The resulting composite material exhibited a gradient in pore width, as determined by image analysis of (iii) scanning electron micrographs. The section numbers in (ii) refer to measurements taken from regions denoted in (iii). Reproduced with permission from [74].

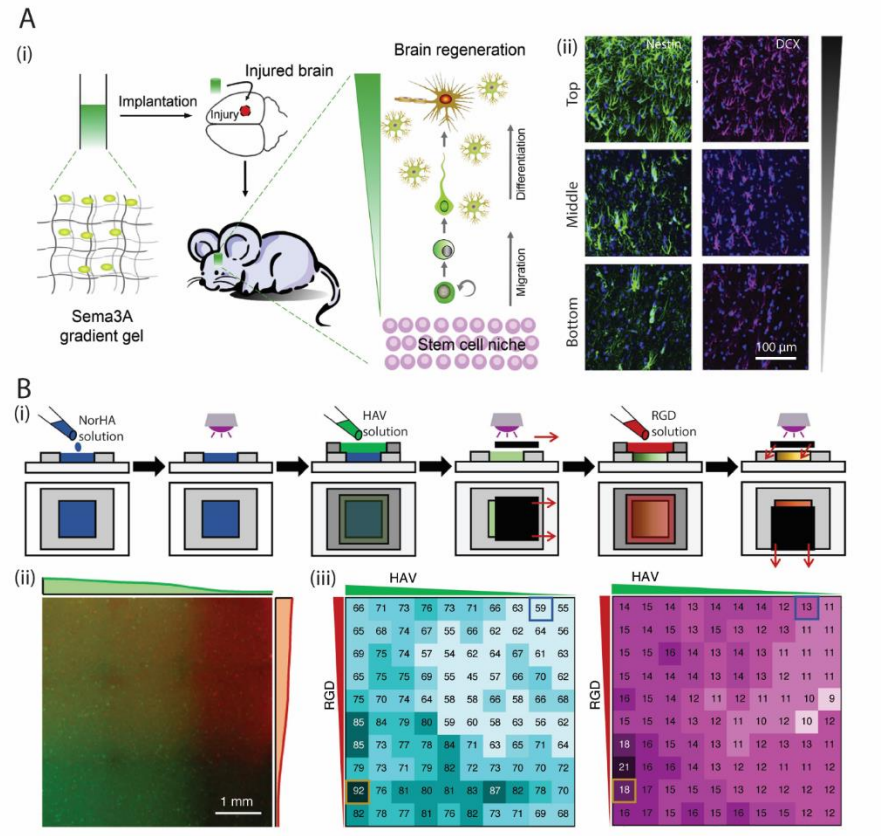

Figure 5. Post-modification to form gradient biomaterials. (A) (i) Gradient biomaterials prepared by the sequential diffusion of a bifunctional crosslinker and Sema3A into a Matrigel hydrogel, and used for *in vivo* implantation. (ii) Fluorescence images showing the distribution of Nestin$^+$ (green) and DCX$^+$ (red) cells that had migrated into different regions of the gradient hydrogels. Reproduced with permission from [80]. (B) (i) Orthogonal gradients formed by sequential photocrosslinking of HAV and RGD peptides, with light exposure controlled using a sliding photomask. (ii) Fluorescence imaging of the orthogonal gradients with rhodamine-labeled RGD (red) and fluorescein-labeled HAV (green). (iii) The orthogonal gradients were shown to regulate the expression of Sox9 (blue) and the synthesis

of aggrecan (purple). Values indicated are based on normalized intensity. Reproduced with permission from [83].

1 **Table 1**. Gradient fabrication strategies and selected examples

ADDITIVE MANUFACTURING	ADVANTAGES	DISADVANTAGES	EXAMPLES	REFERENCES
Layering	• Rapid and simple protocol • No specialist equipment	• Restricted to stepped transitions • Risk of delamination	• Compositional • Mechanical	• [23, 25-28] • [25, 27]
3D Printing	• Freeform control over the material architecture • Can form continuous gradients • Can form a range of gradients	• Requires printable materials • Requires specialist equipment and significant user expertise	• Cellular • Architectural • Mechanical • Compositional	• [46] • [33-40] • [40] • [32, 33, 36, 40, 47-49]
Fluid Mixing	• Rapid and simple protocol • Can form continuous gradients • Can form a range of gradients	• Restricted to single gradients	• Compositional • Biochemical • Mechanical • Architectural	• [52, 55, 56] • [55] • [54] • [57]
Electrospinning	• Rapid and simple protocol • Can form continuous gradients • Can form a range of gradients	• Restricted to thin scaffolds • Challenging with live cells	• Compositional • Architectural • Mechanical	• [60] • [61, 62] • [62]
COMPONENT REDISTRIBUTION	**ADVANTAGES**	**DISADVANTAGES**	**EXAMPLES**	**REFERENCES**
Convection	• Rapid and simple protocol • Can form continuous gradients	• Requires certain geometry and convective conditions	• Compositional • Architectural	• [17, 63, 67] • [63]
Centrifugation	• Rapid and simple protocol • Can form continuous gradients	• Requires a density difference • Restricted to single gradients	• Compositional • Architectural • Morphogen	• [65] • [64] • [65]
Buoyancy	• Rapid and simple protocol • Can form continuous gradients • Can form a range of gradients	• Requires a density difference • Restricted to single gradients	• Compositional • Mechanical • Morphogen	• [66] • [66] • [66]
Magnetic Fields	• Rapid and simple protocol • Can form continuous gradients	• Requires magnetic particles • Risk of particle cytotoxicity	• Cellular • Morphogen	• [68] • [69]
Electric Fields	• Can form continuous gradients	• Requires field responsivity • Risk of electrical cytotoxicity	• Compositional • Mechanical	• [70] • [70]
CONTROLLED PHASE CHANGES	**ADVANTAGES**	**DISADVANTAGES**	**EXAMPLES**	**REFERENCES**
Heat-Induced	• Rapid and simple protocol • Can form continuous gradients	• Requires thermoresponsivity at suitable temperatures	• Architectural • Mechanical	• [74-76] • [73]
Light-Induced	• High resolution • Can form continuous gradients	• Requires photoresponsivity • Risk of cell damage from UV light or free radicals	• Mechanical	• [71, 72, 83]
POST-MODIFICATION	**ADVANTAGES**	**DISADVANTAGES**	**EXAMPLES**	**REFERENCES**
Dipping or Filling	• Rapid and simple protocol • Can form continuous gradients	• Requires relatively rapid binding kinetics	• Compositional	• [77, 78]
Diffusion	• Simple protocol • Can form continuous gradients	• Requires optimized mass transport conditions • Slow fabrication process	• Compositional	• [79, 80]
Light-induced	• High resolution • Can form continuous gradients	• Requires photoresponsivity • Risk of cell damage from UV light or free radicals	• Compositional	• [82-86]

2